

Black and gray solitons in holographic superfluids at zero temperature

Meng Gao*

*Department of Physics, College of Science,
China University of Petroleum, Beijing 102249, China
School of Physical Sciences, University of Chinese
Academy of Sciences, Beijing 100049, China*

Yuqiu Jiao[†]

*Department of Physics, College of Science,
China University of Petroleum, Beijing 102249, China*

Xin Li[‡]

*School of Physical Sciences, University of Chinese
Academy of Sciences, Beijing 100049, China*

Yu Tian[§]

*School of Physical Sciences, University of Chinese
Academy of Sciences, Beijing 100049, China
Institute of Theoretical Physics, Chinese Academy of Sciences, Beijing 100190, China*

Hongbao Zhang[¶]

*Department of Physics, Beijing Normal University, Beijing 100875, China
Theoretische Natuurkunde, Vrije Universiteit Brussel,
and The International Solvay Institutes,
Pleinlaan 2, B-1050 Brussels, Belgium*

Abstract

We construct gray soliton configurations, which move at constant speeds, in holographic superfluids for the first time. Since there should be no dissipation for a moving soliton to exist, we use the simplest holographic superfluid model at zero temperature, considering both the standard and alternative quantizations. For comparison purpose, we first investigate black solitons in the zero temperature holographic superfluids, which are static configurations. Then we focus on the numerical construction of gray solitons under both quantizations, which interpolate between the (static) black solitons and sound waves (moving at the speed of sound). Interestingly, under the standard quantization, a peculiar oscillation of the soliton configurations is observed, very much resembling the Friedel oscillation in fermionic superfluids at the BCS regime. Some implications and other aspects of the soliton configurations are also discussed.

* 2015210214@student.cup.edu.cn

† napoleonest@aliyun.com

‡ lixin615@mails.ucas.edu.cn

§ ytian@ucas.ac.cn

¶ hzhang@vub.ac.be

I. INTRODUCTION AND MOTIVATION

AdS/CFT correspondence states that a gravitational system in the anti-de Sitter space is dual to a conformal field theory on its conformal boundary, realizing the so-called holographic principle[1–3]. The main application of AdS/CFT, or holography, is that it can be used to explore strongly coupled quantum systems, which are outside the reach of conventional perturbative techniques. There are many papers that have applied this correspondence to various condensed matter systems with strong interaction, for example [4–6]. There are also some papers[7–10] that have investigated the features of superfluid, such as turbulence, by means of this correspondence. In applied AdS/CFT, an Abelian Higgs model in the background of an AdS black hole[11, 12] that exhibits spontaneous breaking of the bulk $U(1)$ symmetry has been extensively studied. Due to the principle of AdS/CFT, this broken $U(1)$ symmetry is global on the boundary, so it is more appropriate that one identifies these models as superfluids[13–17]. There are some interesting objects in superfluids, such as vortices and solitons. In [18–22], vortex solutions are studied using the holographic model in [11] (the HHH model). A dark (bright) soliton is an interface of reduced (increased) particle number density between two superfluid phases (for a review, see [23]). Black solitons, which are static dark solitons, in holographic superfluids have been studied in [24, 25]. However, the more general dark solitons, which move at constant speeds and are called gray solitons, as well as bright solitons have not been constructed in holographic models.

In this paper, we are interested in holographic dark soliton solutions at zero temperature, including the static black solitons and the gray solitons moving at constant speeds. This zero temperature holographic setup is realized by an Abelian Higgs model in the AdS soliton background[32], instead of the AdS black hole in [11, 12] for the finite temperature case. Our major motivations to consider the zero temperature holographic superfluids are two-fold. First, it is well known that in fermionic cold atom systems there are two types (or two mechanisms) of superfluidity, i.e. the BEC superfluidity and the BCS superfluidity, with a crossover (called the BEC-BCS crossover) in between[35, 36]. With the Bogoliubov-de Gennes (BdG) equations as a mean field description of the fermionic superfluidity, black soliton configurations in these two types of superfluids are shown to have a salient difference in the (particle number) density depletion at their centers[30]. In the finite temperature holographic superfluids, the authors of [24] have investigated the density depletion at the

centers of the black solitons under two types of quantizations, i.e. the standard quantization and alternative quantization, of the bulk scalar field and argued that these two types of quantizations correspond to the BCS-like and BEC-like superfluids, respectively (see also [31]). However, the BdG analysis in [30] is at zero temperature, and it is numerically difficult to make the temperature of the HHH model used in [24] low enough, which renders the argument of the correspondence between different quantizations and different types of superfluids limited. In order to avoid this limitation, we directly use the zero temperature holographic setup.

Next, since there is dissipation when local structures are traveling in finite temperature (holographic) superfluids[7], moving “solitons” are not expected to preserve their shape under such backgrounds, i.e. we cannot obtain the constantly traveling gray soliton configurations, which is more interesting than black solitons in many aspects. But just like the gray soliton solution to the (zero temperature) Gross-Pitaevskii (GP) equation[37–39], as will be shown in this paper, we can construct gray soliton solutions in the zero temperature holographic superfluids instead. Having these holographic gray solitons at hand, one can extend the study of the holographic BEC-like and BCS-like behaviors mentioned above and the stability of holographic black solitons to the more general cases[34]. One can even investigate the collision of two or more holographic gray solitons and other dynamical properties of them.

The paper is organized as follows. In the next section, we introduce the zero temperature holographic superfluid model. In Sec.III, we first present the black soliton solutions under both quantizations at different chemical potentials. Then we study the density depletion of the black solitons and show the holographic BEC-like and BCS-like behaviors at different quantizations. In Sec.IV, with the help of a “comoving” frame, we construct the gray soliton solutions at different speeds of traveling and investigate their (particle number) density profiles. As one of the key features of gray solitons, we show that the (gauge invariant) phase differences between the condensates on their two sides are not equal to π , in contrast to the case of black solitons, which have phase differences exactly equal to π . Actually, the obtained gray soliton configurations perfectly interpolate between the (static) black solitons and sound waves (moving at the speed of sound). Unexpectedly, for both black solitons and gray solitons under the standard quantization, we can observe peculiar oscillatory behaviors of their configurations, which very much resemble the Friedel oscillation in fermionic superfluids at the BCS limit, further supporting the correspondence proposed by [24]. In the end, we

draw our conclusions and have some discussions.

II. HOLOGRAPHIC SETUP

In this section, we present the holographic model for zero temperature superfluids. The action is based on the Abelian Higgs model[11, 12] that is given by

$$S = \frac{1}{16\pi G} \int_{\mathcal{M}} d^4x \sqrt{-g} \left(R + \frac{6}{L^2} + \frac{1}{e^2} \mathcal{L}_{matter} \right). \quad (1)$$

Here G is Newton's constant, and the Lagrangian for matter fields reads

$$\mathcal{L}_{matter} = -\frac{1}{4} F_{ab} F^{ab} - |D\Psi|^2 - m^2 |\Psi|^2, \quad (2)$$

where $D = \nabla - iA$, $F = dA$, with ∇ the covariant derivative compatible to the metric. e and m are the charge and mass of the complex scalar field Ψ , respectively. To make the model easier, we will work in the probe limit, namely the limit that the backreaction of the matter fields onto the bulk spacetime is neglected. In what follows, we will take the units in which $L = 1$, $16\pi G e^2 = 1$. We just focus on the action of the matter fields which reads

$$S = \int_{\mathcal{M}} d^4x \sqrt{-g} \left(-\frac{1}{4} F_{ab} F^{ab} - |D\Psi|^2 - m^2 |\Psi|^2 \right). \quad (3)$$

In AdS/CFT, a bulk spacetime with a black hole corresponds to a boundary system at finite temperature, with the Hawking temperature of the black hole corresponding to the temperature of the boundary system. But here we would like to investigate the superfluid model under the AdS soliton background[28, 29, 32], which implies the temperature of the holographic superfluids is zero. The metric of the (1+3)D AdS soliton spacetime in the Schwarzschild coordinates, which is just a double Wick rotation of the Schwarzschild-AdS black brane, reads

$$ds^2 = \frac{1}{z^2} \left[-dt^2 + \frac{dz^2}{f(z)} + dx^2 + f(z) d\xi^2 \right]. \quad (4)$$

Here $f(z) = 1 - (\frac{z}{z_0})^3$ with $z = z_0$ the tip where our geometry caps off and $z = 0$ the AdS boundary. In order to make the geometry smooth at the tip, we are required to impose the periodicity $\frac{4\pi z_0}{3}$ onto the ξ coordinate. With the help of the scale invariance[12] and for numerical simplicity, we shall set $z_0 = 1$.

Variation of the action gives rise to the equations of motion for the matter fields, which can be written as

$$\nabla_a F^{ab} = i[\Psi^* D^b \Psi - \Psi (D^b \Psi)^*], \quad (5)$$

$$0 = D_a D^a \Psi - m^2 \Psi. \quad (6)$$

The asymptotical behavior for the bulk fields near the AdS boundary goes as [12, 13]

$$A_\mu = a_\mu + b_\mu z + \dots, \quad (7)$$

$$\Psi = \Psi_- z^{\Delta_-} + \Psi_+ z^{\Delta_+} + \dots. \quad (8)$$

The mass of scalar field is related to the conformal dimension Δ of the condensate as $\Delta_\pm = 3/2 \pm \sqrt{9/4 + m^2}$ [26] in four dimensional bulk spacetime. The condition $m^2 \geq -9/4$ for Δ to be real is known as the Breitenlohner-Freedman (BF) bound [27]. We set $m^2 = -2$ for numerical simplicity in this paper, namely $\Delta_- = 1$ and $\Delta_+ = 2$. In this case there are two choices for the source [12], which are called the standard quantization and the alternative quantization, respectively. According to the holographic dictionary, we can obtain the vacuum expectation of the operators on the boundary as

$$\langle j^\mu \rangle = \frac{\delta S_{onshell}}{\delta a_\mu} = b^\mu, \quad (9)$$

$$\langle O_\pm \rangle = \frac{\delta S_{onshell}}{\delta \Psi_\mp} = \pm \Psi_\pm^*. \quad (10)$$

Here j^μ is the conserved current on the boundary, corresponding to the conserved particle number of the boundary system. Particularly, j^t is the particle number density and $a_t = A_t|_{z=0}$ the chemical potential conjugate to the conserved particle number. The vacuum expectation value of the scalar operator $\langle O_\pm \rangle$ is interpreted as the condensate in the holographic superfluid model. The choice of Ψ_- or Ψ_+ as the source corresponds to the standard or alternative quantization, respectively. If the condensate (or order parameter in the language of Ginzburg-Landau phase transition) is not zero when the source is turned off, the U(1) symmetry is spontaneously broken and the boundary system is in a superfluid phase, otherwise it is in a normal phase. For an equilibrium holographic superfluid, where the configuration is independent of x and ξ , investigation of this phase transition leads to a critical chemical potential μ_c (see [29] for the specific case considered here) for each of the quantizations, beyond which the system will be in the superfluid phase.

In the following, we will focus on the superfluid phase, i.e. the chemical potential μ is above μ_c , and consider the configuration that is inhomogeneous in the x direction. For the sake of solving the equations of motion above, we should first choose the axial gauge $A_z = 0$ for the U(1) gauge fields. For simplicity, we assume that the non-vanishing bulk fields are $\Psi := z\psi$, A_t and A_x , which do not depend on the coordinate ξ . Therefore, the equations of motion become

$$0 = \partial_t^2 \psi + (z + A_x^2 - A_t^2 + i\partial_x A_x - i\partial_t A_t) \psi + 2iA_x \partial_x \psi - 2iA_t \partial_t \psi - \partial_x^2 \psi + 3z^2 \partial_z \psi + (z^3 - 1) \partial_z^2 \psi, \quad (11)$$

$$0 = \partial_t^2 A_x - \partial_t \partial_x A_t - i(\psi \partial_x \psi^* - \psi^* \partial_x \psi) + 2A_x \psi \psi^* + 3z^2 \partial_z A_x + (z^3 - 1) \partial_z^2 A_x, \quad (12)$$

$$0 = (z^3 - 1) \partial_z^2 A_t + 3z^2 \partial_z A_t - \partial_x^2 A_t + \partial_t \partial_x A_x + 2A_t \psi \psi^* + i(\psi^* \partial_t \psi - \psi \partial_t \psi^*), \quad (13)$$

$$0 = \partial_t \partial_z A_t + i(\psi \partial_z \psi^* - \psi^* \partial_z \psi) - \partial_z \partial_x A_x, \quad (14)$$

where the third one can be taken as the constraint equation.

III. BLACK SOLITONS

Now we study the black soliton structure in the zero temperature holographic model. Without loss of generality, we assume that the inhomogeneous direction of the soliton configuration is the x direction. There is a density depletion at some positions between two superfluid phases, where it produces the black soliton structure with the order parameter changing sign across the interface. Therefore, the matter fields are functions of both x and z for (static) black solitons. Namely, $\psi = \psi(z, x)$, $A_t = A_t(z, x)$ and $A_x = A_x(z, x)$. We further recast the complex scalar field ψ in the form $\psi(z, x) = \phi(z, x) \exp[i\varphi(z, x)]$. Then

we substitute ψ , A_t and A_x into equations (11) to (14) and obtain the following equations:

$$0 = (z + A_x^2 - A_t^2) \phi - 2A_x \phi \partial_x \varphi - \partial_x^2 \phi - \phi (\partial_x \varphi)^2 + 3z^2 \partial_z \phi + (z^3 - 1) [\partial_z^2 \phi - \phi (\partial_z \varphi)^2], \quad (15)$$

$$0 = \phi \partial_x A_x + 2A_x \partial_x \phi + 2(\partial_x \phi) \partial_x \varphi + \phi \partial_x^2 \varphi + 3z^2 \phi \partial_z \varphi + (z^3 - 1) [2(\partial_z \phi) \partial_z \varphi + \phi \partial_z^2 \varphi], \quad (16)$$

$$0 = -2\phi^2 \partial_x \varphi + 2A_x \phi^2 + 3z^2 \partial_z A_x + (z^3 - 1) \partial_z^2 A_x, \quad (17)$$

$$0 = (z^3 - 1) \partial_z^2 A_t + 3z^2 \partial_z A_t - \partial_x^2 A_t + 2\phi^2 A_t, \quad (18)$$

$$0 = 2\phi^2 \partial_z \varphi - \partial_z \partial_x A_x. \quad (19)$$

Because we are looking for static soliton solutions, the currents in the holographic system should be zero. The RHS of (5) is zero, namely $j^x = 0 = j^z$, so we have

$$\partial_z \varphi = 0 \quad (20)$$

$$\partial_x \varphi = A_x \quad (21)$$

With the constraint conditions above, (19) and (17) are satisfied automatically. Moreover, we can choose the gauge $A_x = 0$, to fix the local U(1) symmetry. And then we only need to choose $\varphi = 0$ to fix the global U(1) symmetry. As a result, the equations of motion (15) to (19) will be simplified as

$$0 = (z - A_t^2) \phi - \partial_x^2 \phi + 3z^2 \partial_z \phi + (z^3 - 1) \partial_z^2 \phi \quad (22)$$

$$0 = (z^3 - 1) \partial_z^2 A_t + 3z^2 \partial_z A_t - \partial_x^2 A_t + 2\phi^2 A_t \quad (23)$$

In the following, we shall numerically solve these nonlinear differential equations by means of the pseudospectral method[29] and Newton-Raphson iteration.

Ideally, the size of the system in the x direction should be infinite. However, a cutoff is needed to impose for numerical treatments. Consider a box of size $1 \times 2L$ (L is much larger than the healing length of black solitons, so that further increasing L will not affect the structure of black solitons) in the z and x directions. Moreover, there are two kinds of boundary conditions that can be imposed to these equations, corresponding to standard and alternative quantizations, respectively. For the standard quantization, we choose Ψ_- to be the source. Therefore, the boundary conditions are $\psi = 0$ and $A_t = \mu$ at $z = 0$. As a result, the order parameter of superfluid is $\Psi_+ = \partial_z \psi$ at $z = 0$. For the alternative quantization,

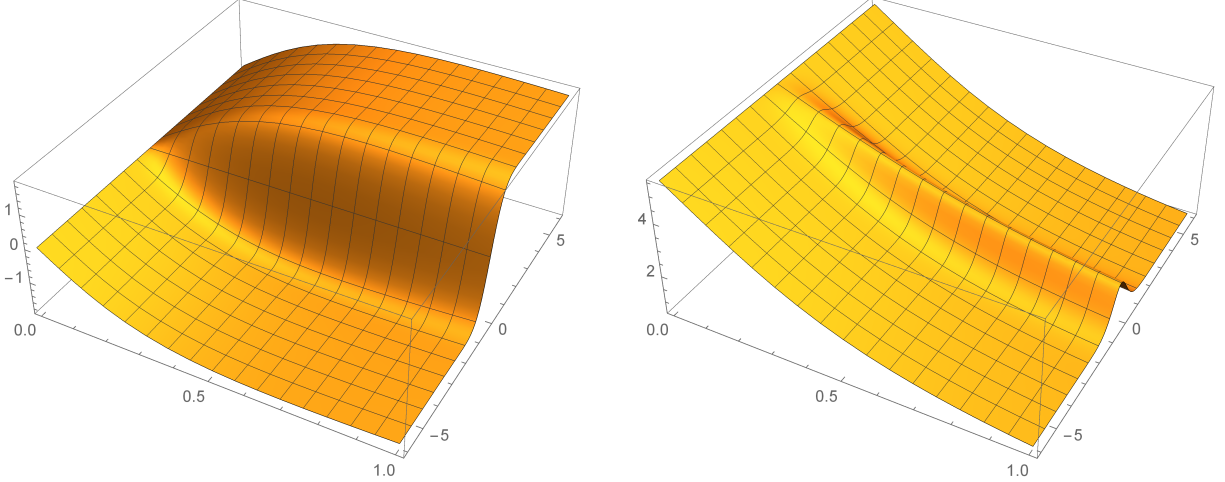


Figure 1. The bulk configurations of the fields $\phi(z, x)$ (left panel) and $A_t(z, x)$ (right panel) for $\mu = 5.5$

the source is taken as Ψ_+ . The boundary condition at $z = 0$ is then $\partial_z \psi = 0$ and $A_t = \mu$. As a result, the order parameter of superfluid is $\langle O \rangle|_{z=0} = \psi$. Taking into account these boundary conditions, we apply the Chebyshev and Fourier pseudospectral methods[29] and Newton iteration to solve the equations. In addition to these boundary conditions in the z direction, we still need the Neumann boundary conditions in the x direction, which are written as $\partial_x \psi = 0$ and $\partial_x A_t = 0$ at both $x = L$ and $x = -L$.

For standard quantization and the chemical potential $\mu = 5.5$, we present the numerical results of the bulk field configurations in Fig.1. The order parameter and density as functions of x are shown in Fig.2. The asymptotical behavior for A_t in the AdS boundary is written as $A_t = \mu - \rho z$. Thus we can read off the charge density as $\rho = -\partial_z A_t|_{z=0}$.

Fig.2 (right panel) shows that there is a density depletion around the centers of the black solitons. As well, the order parameter is zero at the center and dramatically changes around the center. Far away enough (much larger than the characteristic scale set by the so-called healing length) from the cores of the black solitons, the order parameter is homogeneous.

For the alternative quantization, we show the numerical results of the bulk field configurations in Fig.3. The order parameter and particle number density as functions of x are shown in Fig.4.

We note that the density depletion at the soliton core is much deeper in Fig.4 than that in Fig.2. In order to see it more clearly, we present the normalized density profiles in Fig.5.

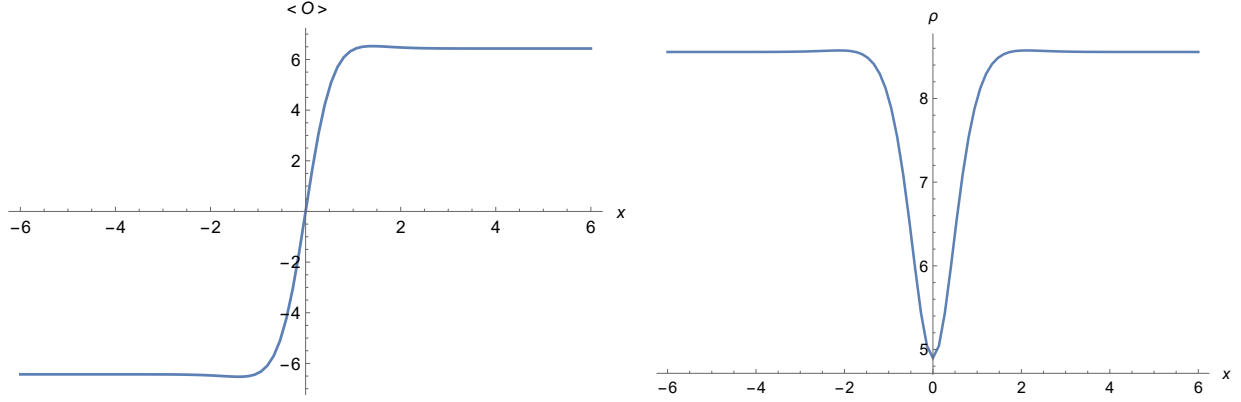


Figure 2. The order parameter (left panel) and particle number density (right panel) with respect to x for $\mu = 5.5$

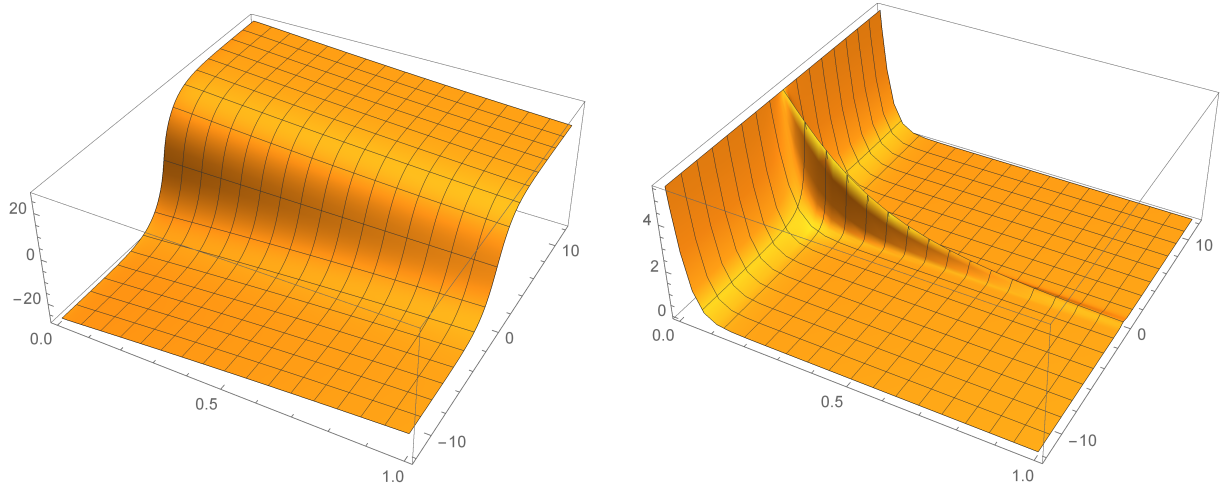


Figure 3. The bulk configurations of the fields $\phi(z, x)$ (left panel) and $A_t(z, x)$ (right panel) for $\mu = 5.5$

We also show the density depletion fraction with respect to the chemical potential (in units of its critical value) in Fig.6 to clarify the difference between the two quantizations. And also ρ_{homo} represents the particle number density in the homogeneous superfluid.

It is interesting to note that the density depletion for holographic solitons is strongly dependent on which type of quantization we choose. In [30], it is shown that the density depletion fraction for solitons from the BdG equations (at zero temperature) is related to whether the system is BEC-type (large depletion) or BCS-type (small depletion). In Fig.6, we note that the density depletion fraction is larger for the alternative quantization than the standard one. In particular, it can be seen that under the large μ/μ_c limit the fraction

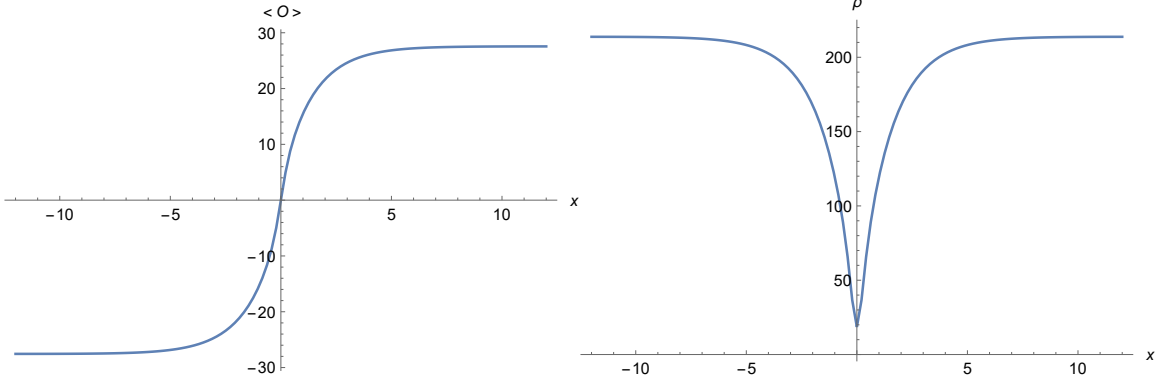


Figure 4. The order parameter (left panel) and particle number density (right panel) with respect to x for $\mu = 5.5$

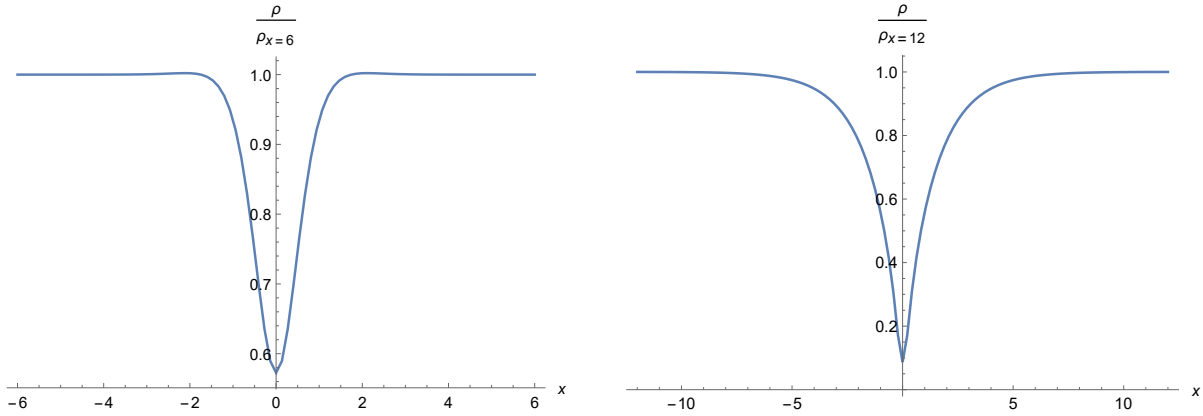


Figure 5. The normalized density profile ($\mu = 5.5$) for the standard quantization (left panel) and the alternative quantization (right panel). The values at the soliton cores are 0.572606 and 0.0866772 for the standard and alternative quantizations, respectively.

ρ_{min}/ρ_{homo} tends to a constant finite value (≈ 0.6) for the standard quantization while it seems to approach zero or some value smaller than 0.1 for the alternative case. Here the relative chemical potential μ/μ_c comes into play because this holographic superfluid model has an extra scale (fixed as $z_0 = 1$ in our discussion) instead of a temperature and the large μ/μ_c limit just means that this extra scale becomes unimportant enough to be neglected, in order not to spoil our comparison with the discussion in [30]. Therefore, we see that the holographic superfluids at the standard and alternative quantizations resemble the BCS-type and BEC-type fermionic superfluids, respectively, consistent with the proposal in[31].

Under the standard quantization, there is another interesting feature of the black soliton

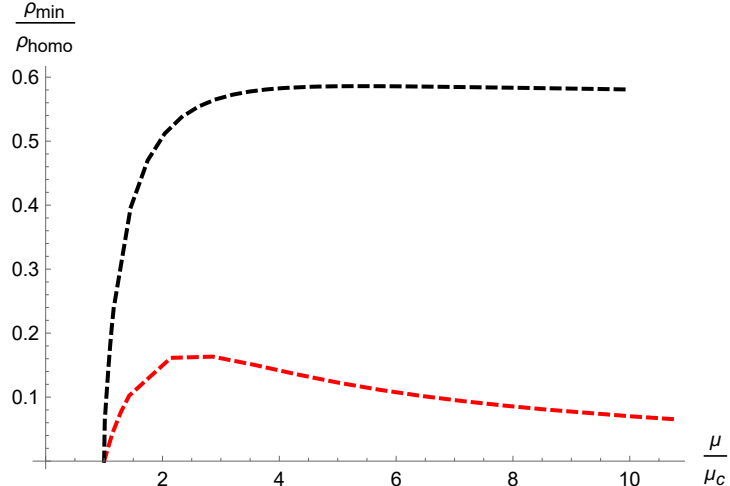


Figure 6. The specific value of density ρ_{min}/ρ_{homo} with respect to the relative chemical potential μ/μ_c for the standard (black dashed) and alternative (red dashed) quantizations.

solutions. Peculiar fluctuations, weak but identifiable, appear around the edges of cliffs of the order parameter and density profiles. In order to further explore the fluctuations, we zoom in on the order parameter and density profiles and present the results in Fig.7 and Fig.8, respectively. These fluctuation behaviors reminds us the Friedel oscillation in the black soliton configurations in the BCS regime of fermionic superfluids[30], which stems from the fact that there are two length scales, the length scale k_F^{-1} corresponding to the Fermi momentum and the coherence length of Cooper pairs, in the BCS-type superfluids. In our case, it is also likely that the fluctuation behaviors result from the interference of two length scales. Moreover, no such fluctuation can be observed under the alternative quantization, even after we zoom in on the order parameter and density profiles, as shown in Fig.9. All these facts appear to be consistent with the proposal in [24]. Additional discussions on the holographic BCS-like configurations can be found in Appendix A.

IV. GRAY SOLITONS

Then we will investigate non-static local structures in superfluids, namely gray solitons, which are really new in the context of holography. In the zero temperature (holographic) superfluids, gray solitons will keep traveling at constant speeds with their shapes exactly preserved.

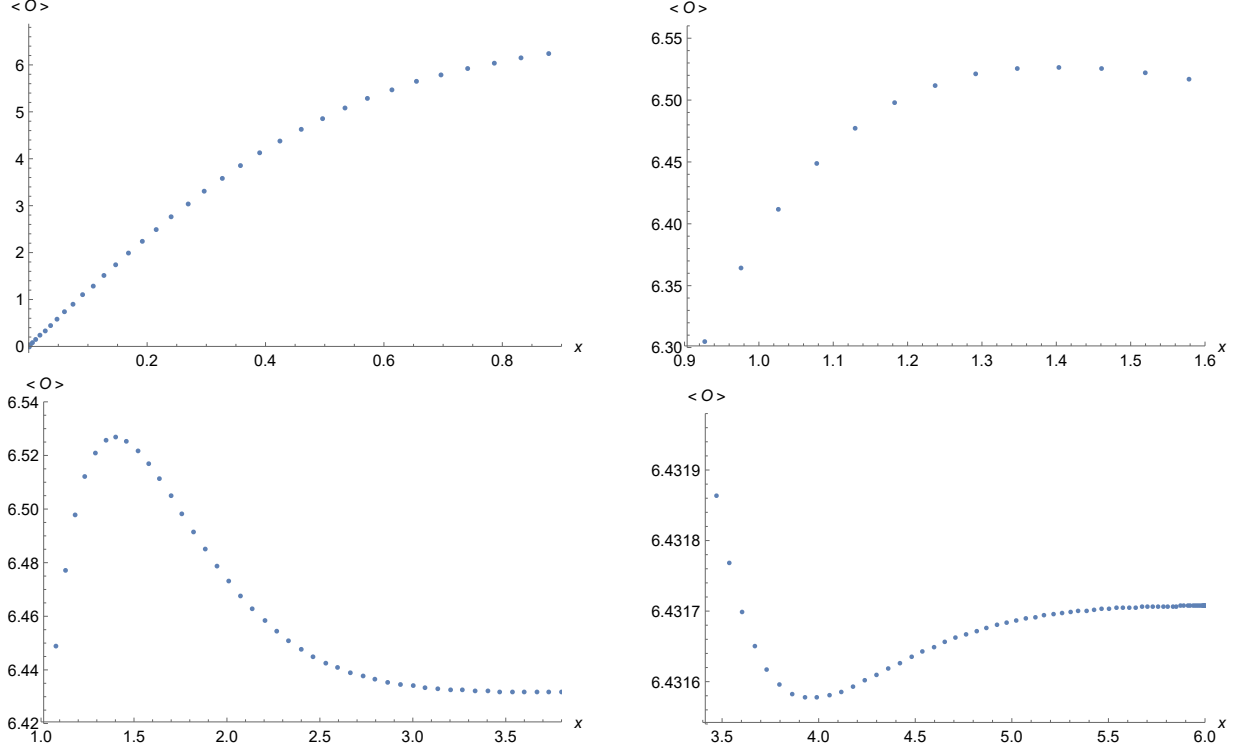


Figure 7. The magnified order parameter, at $\mu = 5.5$, as a function of x from 0 to 6 (half plot of the box) under the standard quantization. It is clearly shown that they have fluctuations.

In order to obtain such kinds of solutions, we take the following useful trick: transforming the original coordinates into the comoving coordinates with respect to a gray soliton. As a result, the gray soliton is static for us in these comoving coordinates. Specifically,

$$\begin{aligned}
 x' &= x - vt, \\
 \psi(z, t, x) &\rightarrow \psi(z, x'), \\
 A_t(z, t, x) &\rightarrow A_t(z, x'), \\
 A_x(z, t, x) &\rightarrow A_x(z, x'),
 \end{aligned} \tag{24}$$

where v is the velocity of the gray soliton, x' is the comoving coordinate and x is the original coordinate (reference frame of the superfluid background).

Then we decompose the complex scalar field ψ into its real part and imaginary part, namely $\psi(x - vt, z) = a(x - vt, z) + ib(x - vt, z)$. Finally the equations of gray solitons

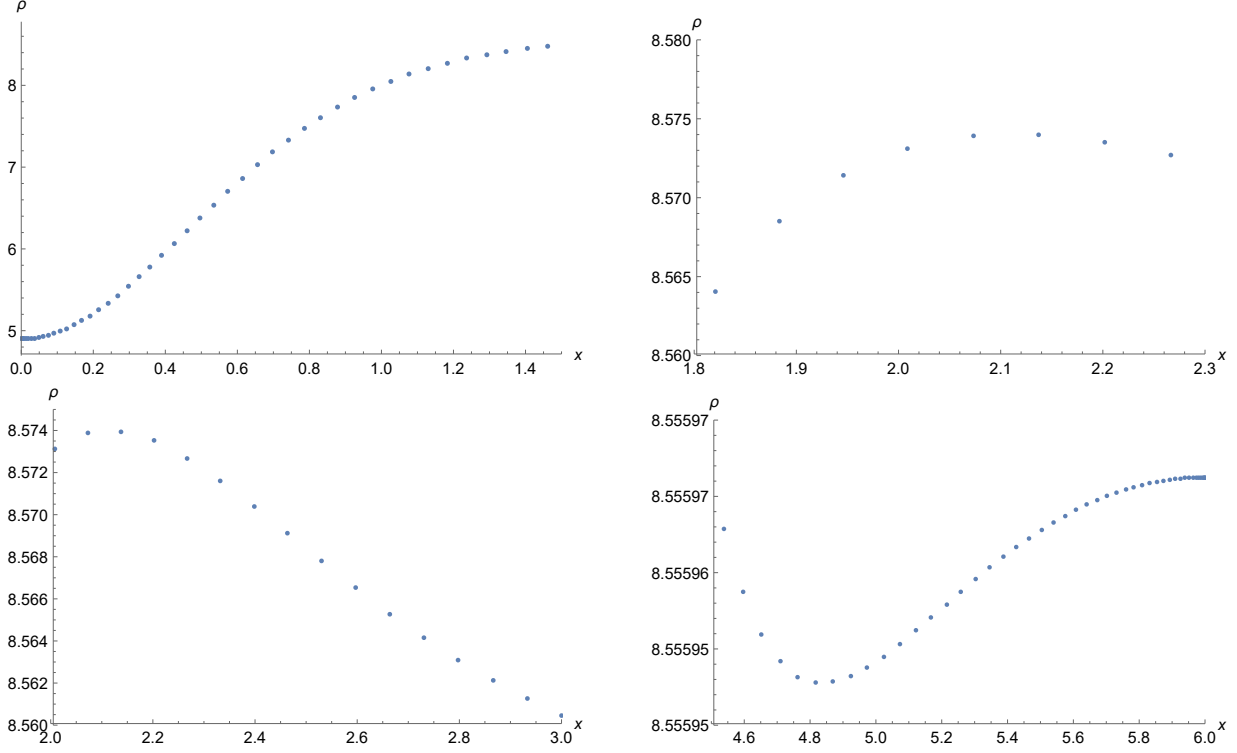


Figure 8. The magnified particle number density, at $\mu = 5.5$, as a function of x from 0 to 6 (half plot of the box) under the standard quantization. It is clearly shown that they have fluctuations.

are written as

$$0 = (v^2 - 1) \partial_x^2 a + a (z + A_x^2 - A_t^2) - b (v \partial_x A_t + \partial_x A_x) - 2A_x \partial_x b - 2v A_t \partial_x b + 3z^2 \partial_z a + (z^3 - 1) \partial_z^2 a, \quad (25)$$

$$0 = (v^2 - 1) \partial_x^2 b + a (v \partial_x A_t + \partial_x A_x) + b (z + A_x^2 - A_t^2) + 2A_x \partial_x a + 2v A_t \partial_x a + 3z^2 \partial_z b + (z^3 - 1) \partial_z^2 b, \quad (26)$$

$$0 = v^2 \partial_x^2 A_x + v \partial_x^2 A_t + 2b \partial_x a - 2a \partial_x b + 2A_x (a^2 + b^2) + 3z^2 \partial_z A_x + (z^3 - 1) \partial_z^2 A_x, \quad (27)$$

$$0 = (z^3 - 1) \partial_z^2 A_t + 3z^2 \partial_z A_t - \partial_x^2 A_t - v \partial_x^2 A_x + 2A_t (a^2 + b^2) + 2va \partial_x b - 2vb \partial_x a, \quad (28)$$

$$0 = -v \partial_z \partial_x A_t + 2a \partial_z b - 2b \partial_z a - \partial_z \partial_x A_x, \quad (29)$$

where the last one can be taken as the constraint equation.

We still impose the same boundary conditions on the equations above as in the black soliton case for ψ and A_t . And we set $A_x|_{x=\pm L} = 0$. The most technical step is to fix the

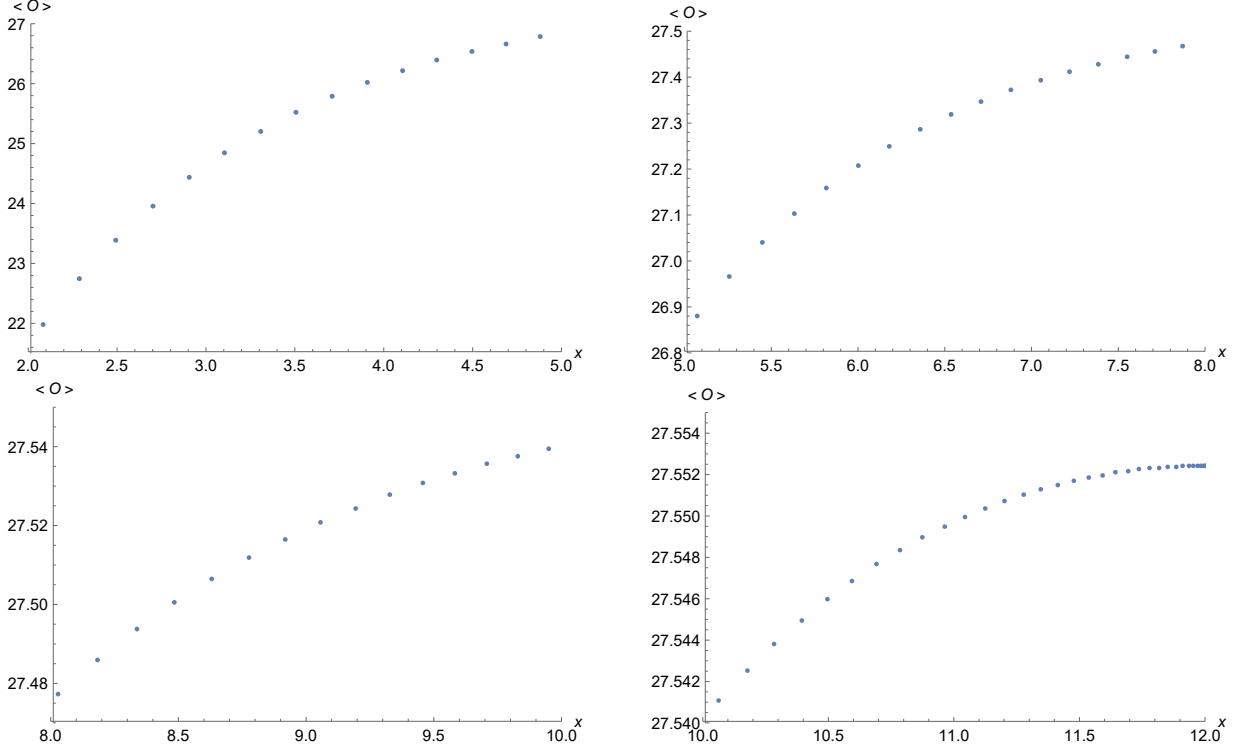


Figure 9. The magnified order parameter under the alternative quantization with the chemical potential $\mu = 5.5$. It can be seen that the order parameter monotonously increases in the x direction.

U(1) gauge. First, we still use the gauge $A_z = 0$. In addition, we will set $A_x(z = 0) = 0$, which makes the local U(1) gauge fixed. Next, we need to fix the global U(1) gauge by imposing the condition $a = 0$ (where $z = 1, x = 0$). Here we also investigate the gray soliton solutions under the standard and alternative quantizations separately.

First of all, we present the condensate and particle number density of gray solitons with different speeds under the standard quantization, which are shown in Fig.10 and Fig.11.

We can see in Fig.10 that the configuration just becomes the black soliton when the speed is zero, and that the depletion of the condensate at the soliton core becomes small with the increase of speed. Eventually, the condensate distribution becomes homogeneous when the soliton speed approaches the speed of sound ($1/\sqrt{2} \approx 0.707$ for the standard quantization[28]), since in this case the moving gray soliton becomes a sound wave, which should actually be a linear perturbation. Meanwhile, the analogous tendency arises in the density distribution, as shown in Fig.11. Similarly, it becomes homogeneous when the soliton speed reaches the speed of sound. Most importantly, the peculiar fluctuations similar to the

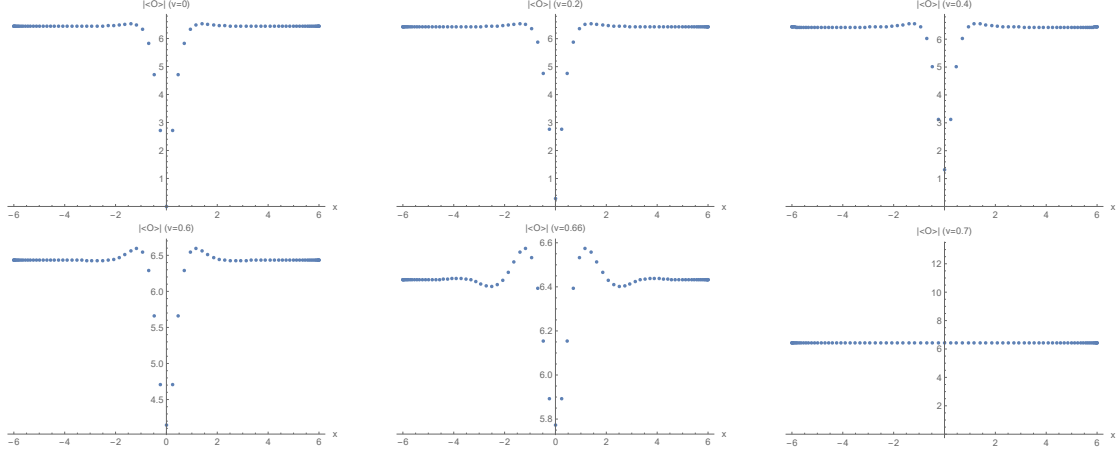


Figure 10. The order parameter $|\langle O \rangle|$ distributions at different speeds ($v = 0, 0.2, 0.4, 0.6, 0.66, 0.7$) of gray solitons with the chemical potential $\mu = 5.5$ at standard quantization. The values of $\frac{|\langle O \rangle|_{x=0}}{|\langle O \rangle|_{x=6}}$ are in sequence 0, 0.0443334, 0.204758, 0.644198, 0.897435, 1 with the increasing velocities.

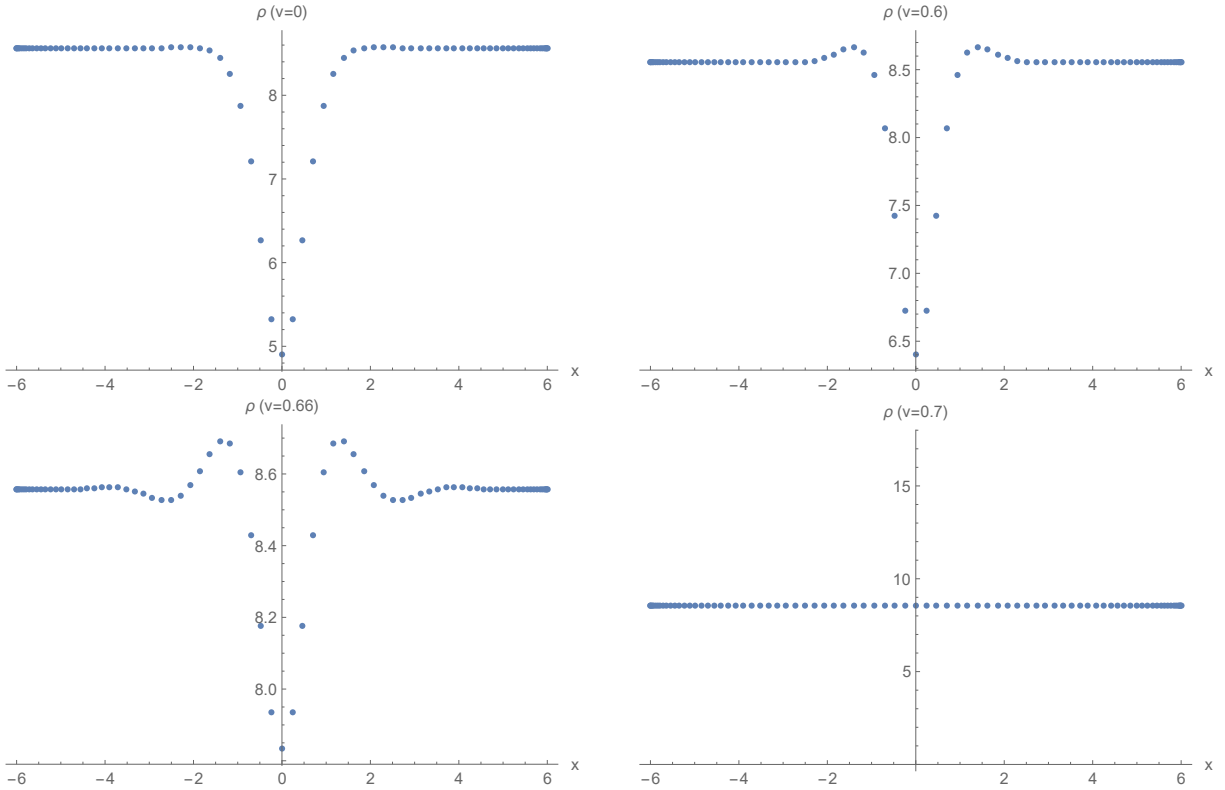


Figure 11. The distributions of particle number density at different speeds ($v = 0, 0.6, 0.66, 0.7$) of gray solitons with the chemical potential $\mu = 5.5$ at standard quantization. The values of $\frac{\rho_{x=0}}{\rho_{x=6}}$ are in sequence 0.572601, 0.74807, 0.915534, 1 with the increasing velocities.

black soliton case also occur in the general gray soliton case, and they become even more remarkable when the soliton speed increases. This enhancement of the Friedel-like oscillation is probably due to the fact that the oscillation amplitude is less sensitive to the change of the soliton speed than the depletion of the soliton configurations are, while in the zero or low speed case the steep variation of the soliton configuration tends to overwhelm the Friedel-like oscillation. Additional discussions on these BCS-like configurations can be found in Appendix B.

It is well known that the phase difference between the condensates on the two sides of a black soliton is π , which is not the case for gray solitons. For the purpose of verifying the gray soliton configurations above, we investigate the gauge invariant phase differences with respect to the soliton speeds. This gauge invariant phase difference is written as $\theta|_{-L}^L - \int_{-L}^L A_x dx$, where θ is the argument of the order parameter of a gray soliton. We present the phase differences and phase distributions in Fig.12 and Fig.13, respectively.

As can be seen from Fig.12 and Fig.13, the absolute value of the phase difference is approximately π when the speed is 0.001, which exactly indicates that the solution becomes a black soliton when the speed is very small. Then the absolute value of the phase difference becomes smaller and smaller when the soliton speed increases. When the soliton speed approaches the speed of sound, the phase difference tends to zero and the phase of the condensate is actually a constant. All these features are expected for gray soliton configurations.

Then we will present the gray soliton solutions under the alternative quantization. The condensate and particle number density are studied as in the case of standard quantization and shown in Fig.14 and Fig.15.

It can be seen that there is no fluctuation around the edges of cliffs of the condensate and density profiles at alternative quantization. The results are consistent with the proposal that the holographic superfluid under the alternative quantization is a BEC-like superfluid. While the speed of sound is $1/\sqrt{3} \approx 0.577$ [28] in the case of alternative quantization.

Again, we also present the phase differences and phase distributions for gray solitons under the alternative quantization in Fig.16. The qualitative behavior of them is the same as in the case of standard quantization.

For comparison with the black soliton case, we also present the density depletion of the gray solitons under both quantizations in Fig.17. It is obvious that the value of $\frac{\rho_{min}}{\rho_{homo}}$ for the

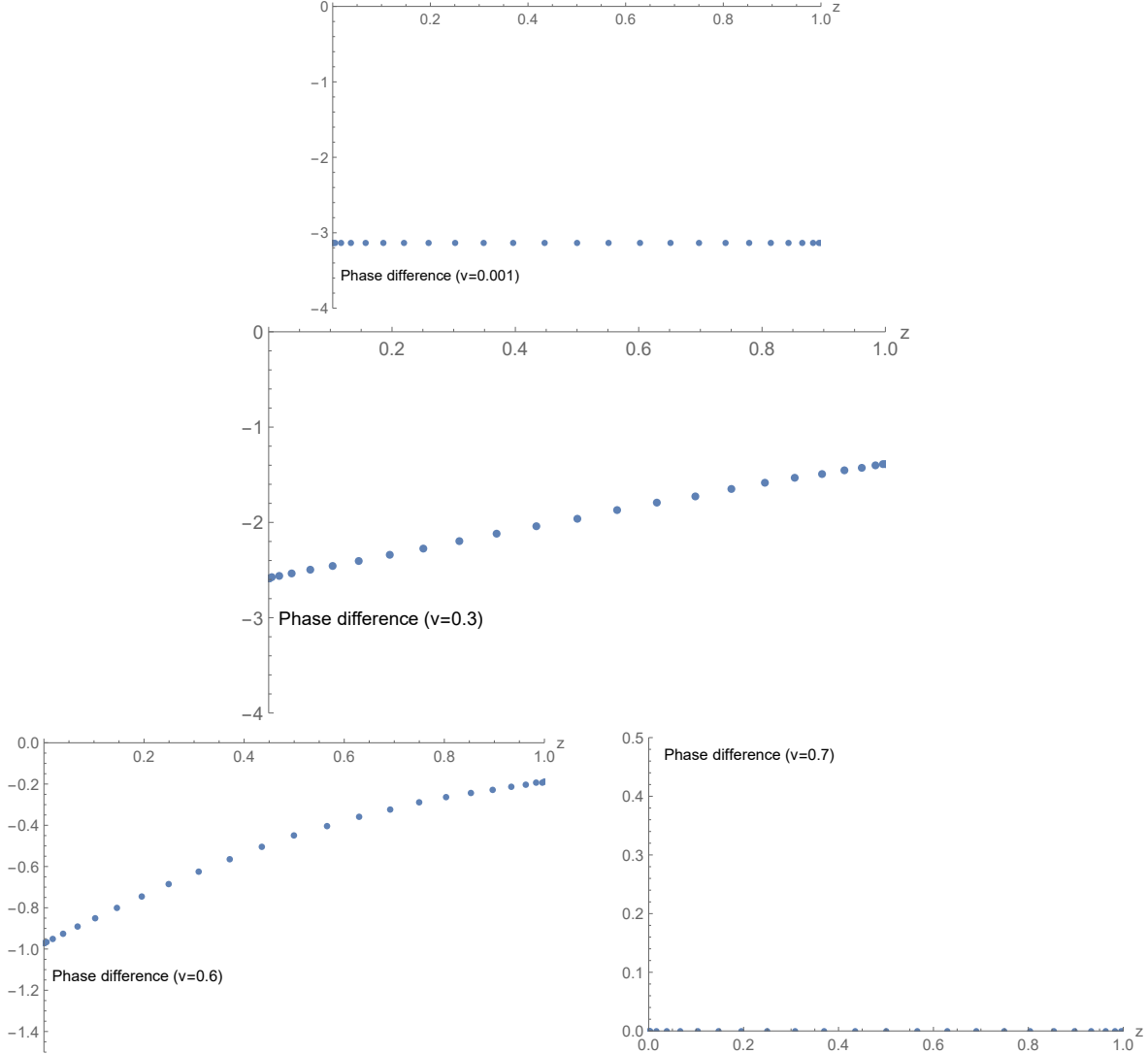


Figure 12. The phase differences at different speeds, under the standard quantization with the chemical potential $\mu = 5.5$.

standard quantization is in general larger than that for the alternative one. Moreover, the difference of density depletion for the two quantizations becomes smaller when the soliton speed increases.

V. SUMMARY AND DISCUSSION

For the zero temperature holographic superfluid model, we have numerically solved the spatially inhomogeneous equations of motion to obtain the black and gray soliton solutions under both the standard and alternative quantizations, and have investigated in detail var-

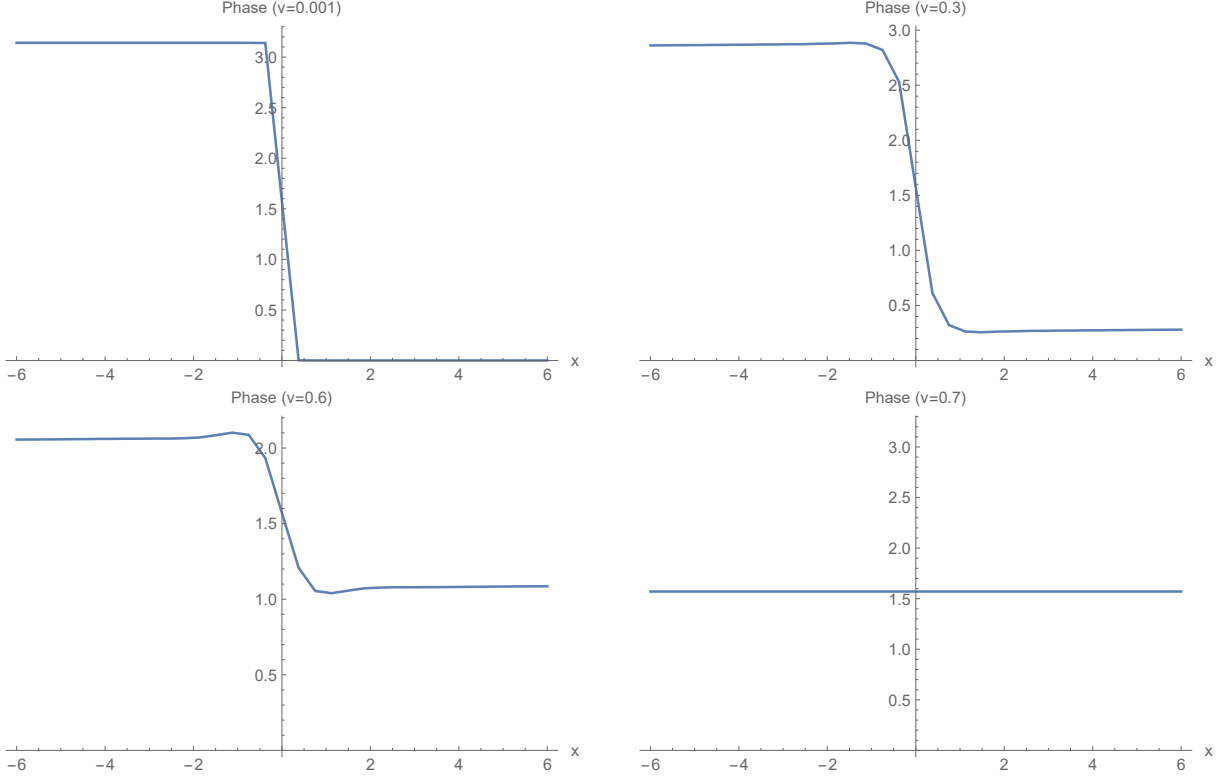


Figure 13. The distributions of phase at different soliton speeds, under the standard quantization with the chemical potential $\mu = 5.5$.

ious aspects of these holographic superfluid solitons.

The simplest such solitary solutions are the black solitons, which are static superfluid structures. After having constructed the holographic black soliton solutions, we focus on the particle number density depletions at the centers of the solitons for the standard and alternative quantizations at different chemical potentials, especially the limit of large chemical potential. As a result, we find that the density depletion is much larger under the alternative quantization than that under the standard one. Our holographic model is a genuine zero temperature superfluid system, so this result acts as a strong support for the correspondence between different quantizations in holography and different types of fermionic superfluids proposed in [24]. Specifically, the alternative quantization corresponds to a BEC-like superfluid, while the standard quantization corresponds to a BCS-like superfluid. Moreover, under the standard quantization there are extra fluctuations, compared to the alternative case, in the black soliton configurations, which resemble the Friedel oscillation in the case of BCS superfluids and further support the above proposal.

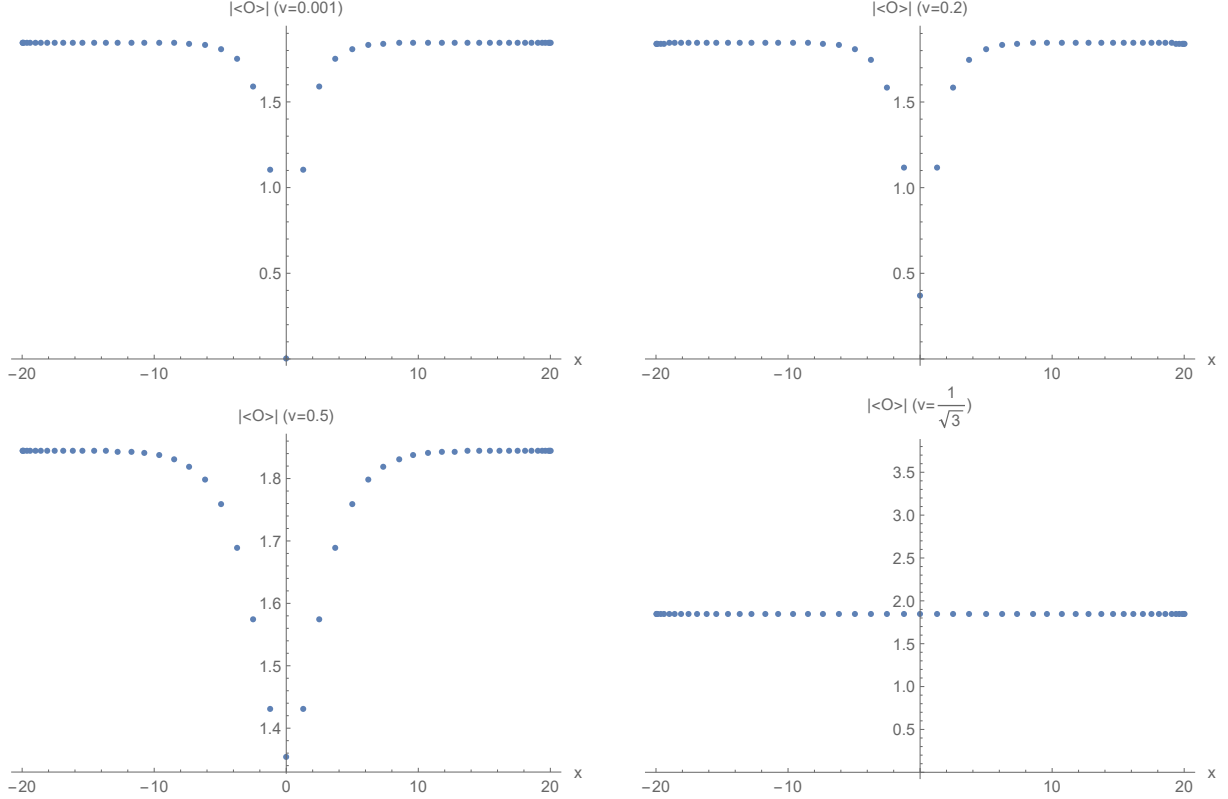


Figure 14. The condensate distributions at various soliton speeds ($v = 0.001, 0.2, 0.5, 1/\sqrt{3}$) under the alternative quantization with the chemical potential $\mu = 1.4$. The values of $\frac{|\langle O \rangle|_{x=0}}{|\langle O \rangle|_{x=20}}$ are in sequence 0.000959, 0.200329, 0.73415, 1 with the increasing velocities.

Then we have investigated the more complicated solitary solutions, the gray solitons, which keep moving at constant speeds. It is shown that these solutions perfectly interpolate between the (static) black solitons and sound waves (moving at the speed of sound). We also find that the density depletion is evidently larger under the alternative quantization than that under the standard one at general soliton speeds. The Friedel-like oscillation under the standard quantization is even more remarkable in the gray soliton case, probably because the oscillation amplitude is less suppressed at higher soliton speed than the condensate variation itself. Finally, we have computed the gauge invariant phase differences between the condensates on the two sides of our holographic gray solitons and verified that these configurations do have all the expected features of gray solitons.

For simplicity, we do not consider the backreaction of the matter fields onto the bulk geometry in our holographic superfluid model. But for a full holographic duality, such backreaction should be taken into account[12]. It is known that black solitons at finite temper-

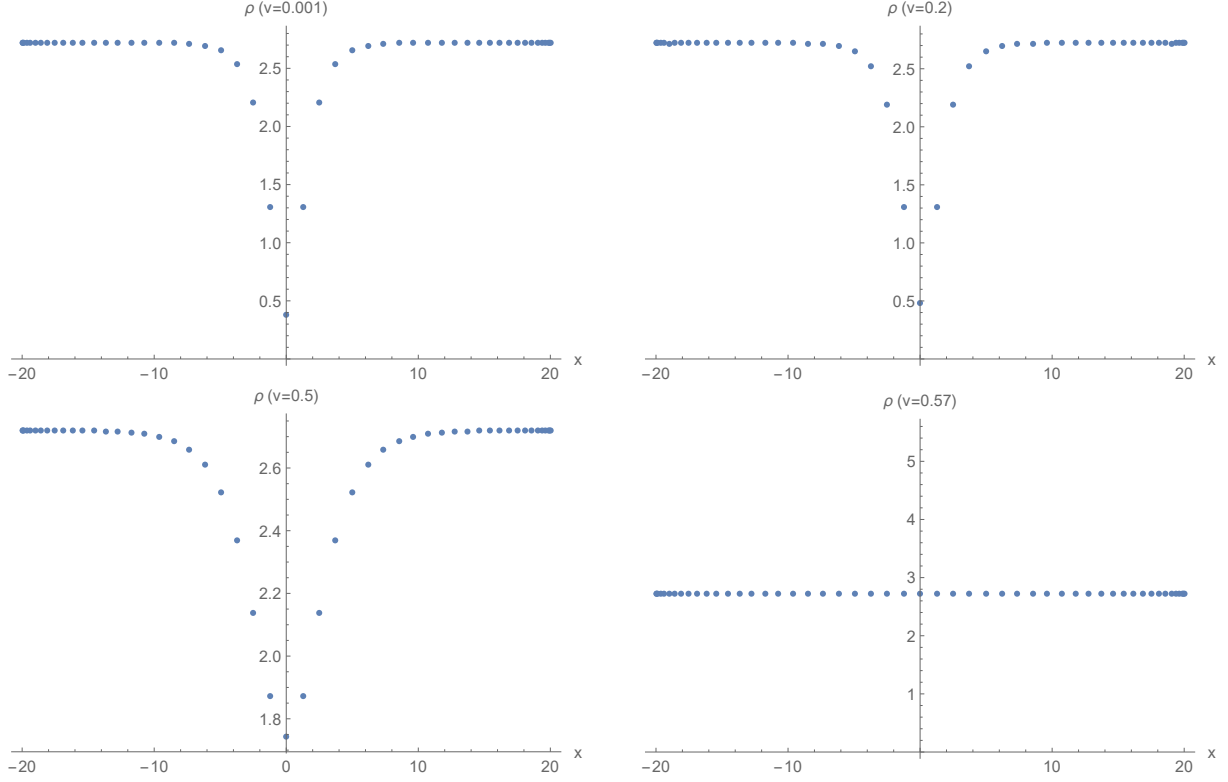


Figure 15. The density distributions at various soliton speeds ($v = 0.001, 0.2, 0.5, 0.57$) under the alternative quantization with the chemical potential $\mu = 1.3$. The values of $\frac{\rho_{x=0}}{\rho_{x=20}}$ are in sequence 0.140459, 0.176112, 0.641066, 1 with the increasing velocities.

ature are unstable against the so-called self-acceleration and snake instabilities, so a natural question is whether it is also the case for the black and gray solitons at zero temperature[34]. It will be also interesting to investigate the collision dynamics of holographic gray solitons. In order to do that, one has to transform the gray soliton solution obtained here in the comoving frame back to the original frame, manage to combine two or more gray solitons as an initial configuration, and then perform the numerical time evolution similar to that in the black hole backgrounds[7, 9, 10]. These topics are left for future exploration.

ACKNOWLEDGMENTS

This work is partially supported by NSFC with Grant No.11475179 and No.11675015. YT is also supported by the "Strategic Priority Research Program of the Chinese Academy of Sciences" with Grant No.XDB23030000. HZ is supported in part by FWOVlaanderen

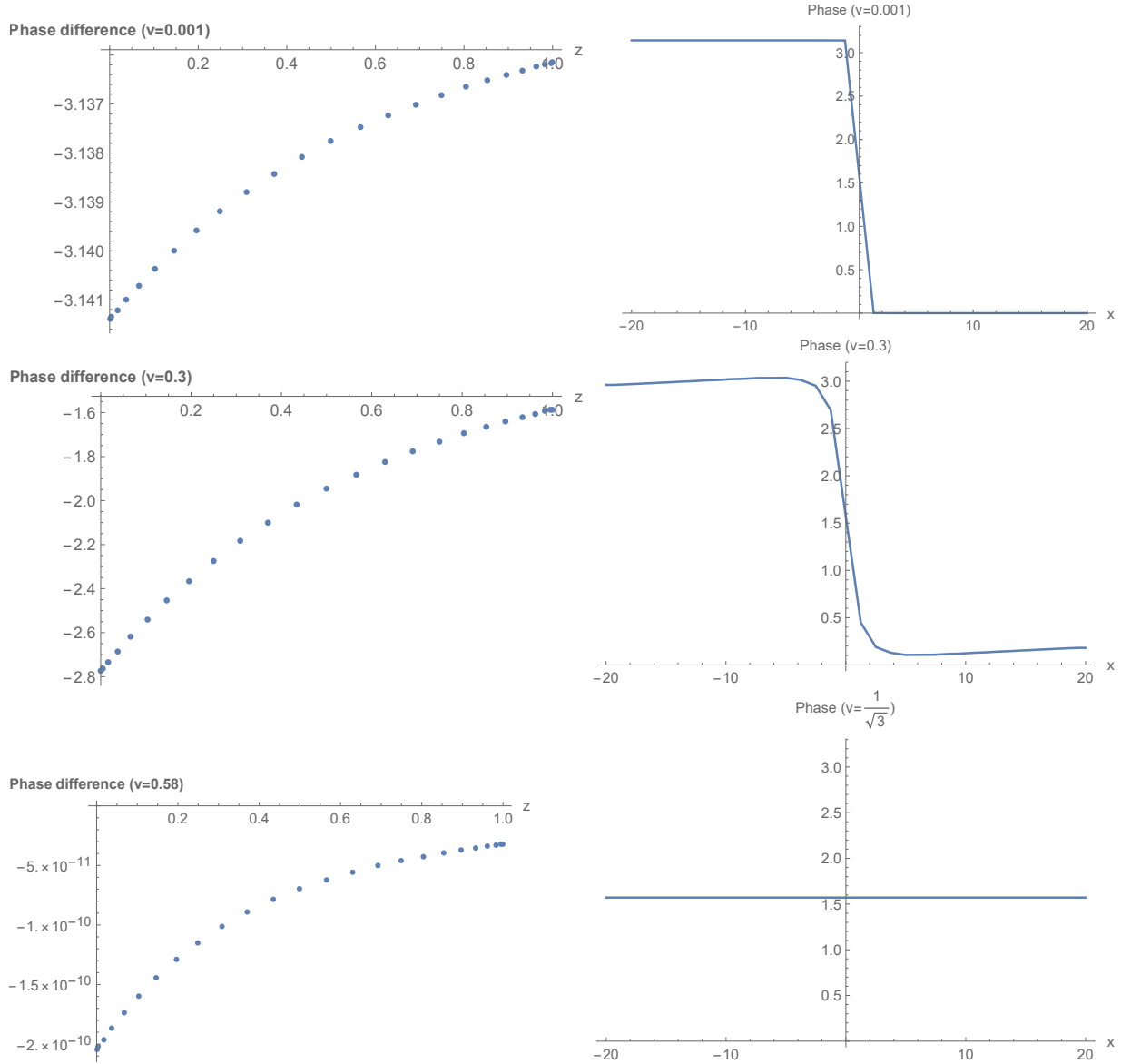


Figure 16. The phase differences and phase distributions for gray solitons at different speeds, under the alternative quantization with the chemical potential $\mu = 1.4$.

through the project G006918N, and by the Vrije Universiteit Brussel through the Strategic Research Program “High-Energy Physics”. He is also an individual FWO fellow supported by 12G3515N.

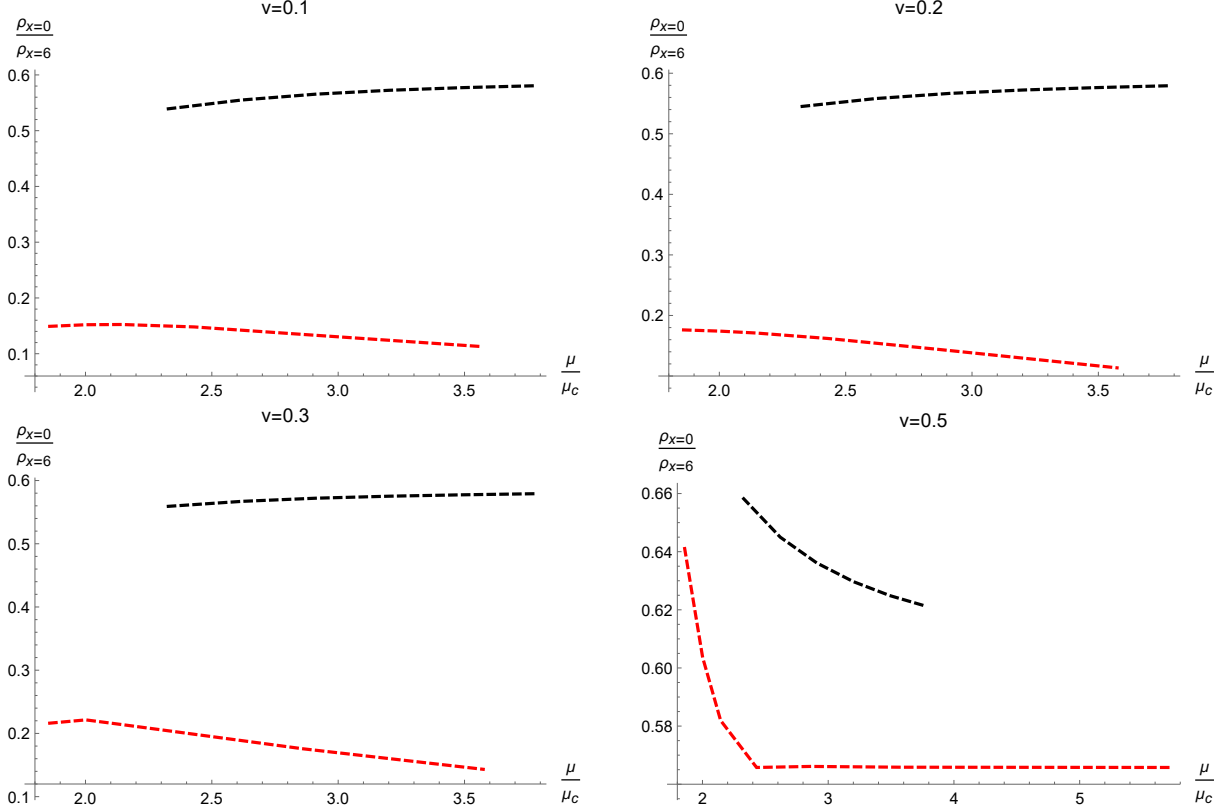


Figure 17. The specific values of density $\frac{\rho_{min}}{\rho_{homo}}$ at different speeds ($v = 0.1, 0.2, 0.3, 0.5$) with respect to the relative chemical potential μ/μ_c for the standard (black dashed) and alternative (red dashed) quantizations.

Appendix A: Fitting of the holographic BCS-like black soliton configurations

We have tried to fit the order parameter and density profiles under the standard quantization with some test functions, as shown in Fig.18. The fitting function for the order parameter is $6.43266 \tanh(x/0.562785) + e^{-(0.884565x)^2} \sin(x/1.3096)$, where 6.43266 is the condensate for a homogeneous solution with the same chemical potential, and 0.562785 is the healing length of the soliton. The fitting function for the charge density is $-3.66259 \text{sech}^2(x/0.676006) + 8.55664 + e^{-(0.802144x)^2} \sin^2(x/1.94947)$, where 0.676006 is the healing length of the soliton, and 3.66259 is the charge density depletion. One remarkable difference, compared to the result in [25], is that both fitting functions have additional terms, reflecting the fluctuation behaviors.

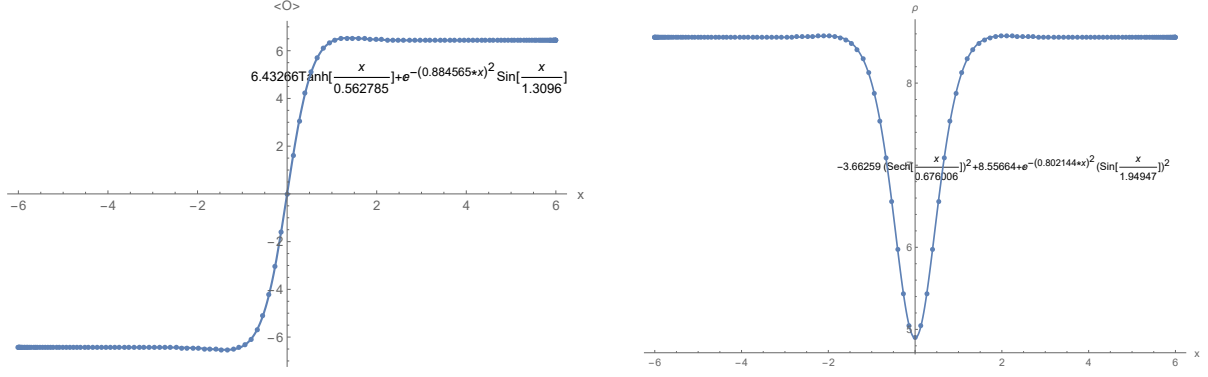


Figure 18. The fitting functions of order parameter (left panel) and charge density (right panel) at standard quantization with the chemical potential $\mu = 5.5$.

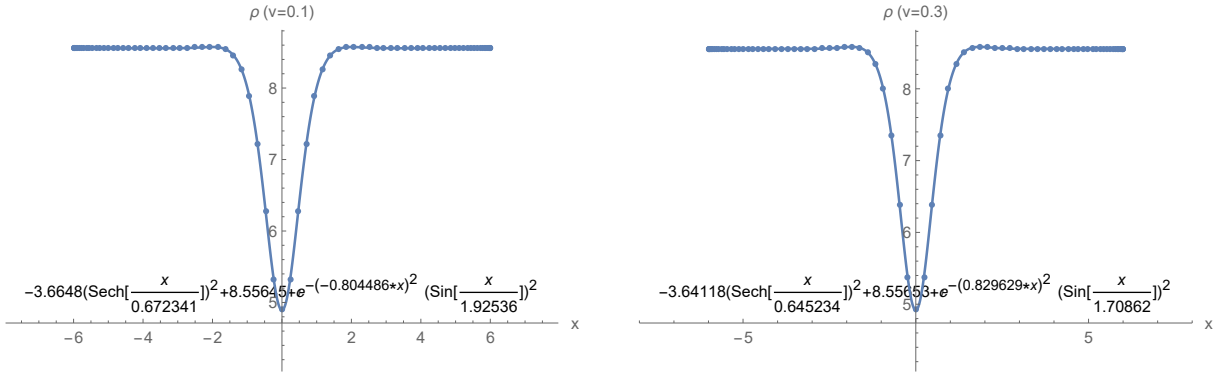


Figure 19. The fitting results, at $\mu = 5.5$, for the density with different speeds under the standard quantization.

Appendix B: Fitting of the holographic BCS-like gray soliton configurations

For the sake of presenting the fluctuations in detail, we have tried to fit the particle number density by functions. The result is shown in Fig.19.

-
- [1] L. Susskind, *Journal of Mathematical Physics*, 36, 6377 (1995).
 - [2] J. Maldacena, *The Large N Limit of Superconformal Field Theories and Supergravity*, *American Institute of Physics*, (1999).
 - [3] S. S. Gubser, I. R. Klebanov and A. M. Polyakov, *Gauge Theory Correlators from Non-Critical String Theory*, *Physics Letters B* (1998).

- [4] S. Sachdev and M. Mueller, *Quantum criticality and black holes*, *Journal of Physics: Condensed Matter*, 21(2009):164216.
- [5] S. A. Hartnoll, *Lectures on holographic methods for condensed matter physics*, *Classical and Quantum Gravity*, 26(2009):224002.
- [6] C. P. Herzog, *Lectures on Holographic Superfluidity and Superconductivity*, *Journal of Physics A Mathematical & Theoretical* 42(2009):343001.
- [7] A. Adams, P. M. Chesler and H. Liu, *Holographic Vortex Liquids and Superfluid Turbulence*, *Science* 341(2013),368-372.
- [8] C. Ewerz, T. Gasenzer, M. Karl and A. Samberg, *Non-thermal fixed point in a holographic superfluid*, *Journal of High Energy Physics* 5(2014):70.
- [9] Y.-Q. Du, C. Niu, Y. Tian and H.-B. Zhang, *Holographic Thermal Relaxation in Superfluid Turbulence*, *Journal of High Energy Physics* 12(2015),1-12.
- [10] S. Lan, Y. Tian and H. Zhang, *Journal of High Energy Phys.* 07 (2016) 092.
- [11] S. A. Hartnoll, C. P. Herzog, and G. T. Horowitz, *Building a holographic superconductor*, *Physical Review Letters* 101(2008):031601.
- [12] S. A. Hartnoll, C. P. Herzog, and G. T. Horowitz, *Holographic Superconductors*, *Journal of High Energy Physics* 12(2008):1-22.
- [13] C. P. Herzog, P. K. Kovtun D. T. Son, *Holographic model of superfluidity*, *Physical Review D* 79(2009):066002.
- [14] O. Domenech, M. Montull, A. Pomarol, et.al., *Emergent Gauge Fields in Holographic Superconductors*, *Journal of High Energy Physics* 08(2010):33.
- [15] A. Salvio, *Superconductivity, Superfluidity and Holography*, *Conf Ser* 442(2013),8378-8387.
- [16] A. Salvio, *Holographic superfluids and superconductors in dilaton-gravity*, *Journal of High Energy Physics* 09(2012):134.
- [17] A. Salvio, *Transitions in Dilaton Holography with Global or Local Symmetries*, *Journal of High Energy Physics* 03(2013):136.
- [18] T. Albash and C. V. Johnson, *A Holographic Superconductor in an External Magnetic Field*, *Journal of High Energy Physics*, 09(2008):1619-1633.
- [19] A. Tameem, and C. V. Johnson, *Vortex and droplet engineering in a holographic superconductor*, *Physical Review D* 80(2009):126009.

- [20] M. Montull, A. Pomarol and P. J. Silva, *Holographic Superconductor Vortices*, *Physical Review Letters* 103(2009),091601.
- [21] K. Maeda, M. Natsuume and T. Okamura, *Vortex lattice for a holographic superconductor*, *Physical Review D* 81(2010),026002.
- [22] V. Keranen, et al., *Inhomogeneous structures in holographic superfluids. II. Vortices*, *Physical Review D* 81(2010),126012.
- [23] Y. S. Kivshar and B. L. Davies, *Dark optical solitons: physics and applications*, *Physics Reports* 298(1998),81-197.
- [24] V. Keranen, E. Keski-Vakkuri, S. Nowling, et.al., *Inhomogeneous Structures in Holographic Superfluids: I. Dark Solitons*, *Phys. Rev. D* 81(2010),126011.
- [25] S.-Q. Lan, W. Liu and Y. Tian, *Statical Structures of the BCS-like Holographic Superfluid in AdS₄ Spacetime*, *Phys. Rev. D* 95(2017),066013.
- [26] I. R. Klebanov and E. Witten, *AdS/CFT correspondence and symmetry breaking*, *Nuclear Physics B* 556.1(1999),89-114.
- [27] P. Breitenlohner and D. Z. Freedman, *Positive Energy in anti-De Sitter Backgrounds and Gauged Extended Supergravity*, *Physics Letters B* 115.3(1982),197-201.
- [28] M.-Y. Guo, S. Lan, C. Niu, Y. Tian and H.-B. Zhang, *Note on Zero Temperature Holographic Superfluids*, *Classical & Quantum Gravity* 33(2016):127001.
- [29] M.-Y. Guo, C. Niu, Y. Tian and H.-B. Zhang, *Modave Lectures on Applied AdS/CFT with Numerics*, (2016) [arXiv:1601.00257].
- [30] M. Antezza, F. Dalfovo, L. P. Pitaevskii and S. Stringari, *Dark solitons in a superfluid Fermi gas*, *Physical Review A* 76(2007):043610.
- [31] O. Dewolfe, O. Henriksson and C.-L. Wu, *A holographic model for pseudogap in BCS–BEC crossover (I): Pairing fluctuations, double-trace deformation and dynamics of bulk bosonic fluid*, *Annals of Physics* 387(2017):75-120.
- [32] T. Nishioka, S. Ryu, and T. Takayanagi, *Holographic Superconductor/Insulator Transition at Zero Temperature*, *Journal of High Energy Physics* 03(2010):131.
- [33] Q.-Y. Pan et al, *Holographic superconductors with various condensates in Einstein-Gauss-Bonnet gravity*, *Physical Review D* 81 (2010):106007.
- [34] M.-Y. Guo, E. Keski-Vakkuri, H. Liu, Y. Tian, and H.-B. Zhang, *Decay of dark solitons and a non-equilibrium dynamical phase transition*, [arXiv:1810.11424].

- [35] M. Randeria, *In Bose-Einstein Condensation*, edited by A. Griffin, D. Snoke, and S. Stringari (Cambridge University Press, Cambridge, 1995):355 – 392.
- [36] E. Timmermans, et.al., *Prospect of creating a composite fermi/bose superfluid*, *Physics Letters A* 285.3(2001):228-233.
- [37] E.P. Gross, *Nuovo Cimento*. 20, 454 (1961).
- [38] L. P. Pitaevskii, *Zh. Eksp. Teor. Fiz.* 40, 646 (1961).
- [39] E. P. Gross, *Hydrodynamics of a Superfluid Condensate*, *Journal of Mathematical Physics* 4.2(1963):195-207.